Permeation of Ammonia Across Bilayer Lipid Membranes Studied by Ammonium Ion Selective Microelectrodes

Yuri N. Antonenko,* Peter Pohl,# and Gennady A. Denisov#
*A. N. Belozersky Institute of Physico-Chemical Biology, Moscow State University, Moscow 119899, Russia, and #Martin-Luther-Universität, Medizinische Fakultät, Institut für Medizinische Physik und Biophysik, 06097 Halle, Germany

ABSTRACT Ammonium ion and proton concentration profiles near the surface of a planar bilayer lipid membrane (BLM) generated by an ammonium ion gradient across the BLM are studied by means of microelectrodes. If the concentration of the weak base is small compared with the buffer capacity of the medium, the experimental results are well described by the standard physiological model in which the transmembrane transport is assumed to be limited by diffusion across unstirred layers (USLs) adjacent to the membrane at basic pH values ($pH > pK_a$) and by the permeation across the membrane itself at acidic pH values. In a poorly buffered medium, however, these predictions are not fulfilled. A pH gradient that develops within the USL must be taken into account under these conditions. From the concentration distribution of ammonium ions recorded at both sides of the BLM, the membrane permeability for ammonia is determined for BLMs of different lipid composition (48×10^{-3} cm/s in the case of diphytanoyl phosphatidylcholine). A theoretical model of weak electrolyte transport that is based on the knowledge of reaction and diffusion rates is found to describe well the experimental profiles under any conditions. The microelectrode technique can be applied for the study of the membrane permeability of other weak acids or bases, even if no microsensor for the substance under study is available, because with the help of the theoretical model the membrane permeability values can be estimated from pH profiles alone. The accuracy of such measurements is limited, however, because small changes in the equilibrium constants, diffusion coefficients, or concentrations used for computations create a systematic error.

INTRODUCTION

The transport of weak electrolytes across cellular and subcellular membranes plays an important role in the cellular metabolism (Jackson, 1987). The studies devoted to the diffusion of weak acids and bases across planar lipid bilayer membranes show the role of the unstirred layers in the immediate membrane vicinity in the process of permeation (Gutknecht and Tosteson, 1973). In spite of the fact that the neutral form of salicylic acid predominates in its transmembrane diffusion, the total acid flux is shown to increase with the increase of the concentration of the anionic form of the acid (Gutknecht and Tosteson, 1973). This result is discussed as evidence in favor of proton transfer reactions proceeding in the unstirred layers of the membrane. The model involving these reactions explains well the pH dependence of the weak electrolyte fluxes. Thus it is used to determine their membrane permeabilities (Walter and Gutknecht, 1986; Xiang and Anderson, 1993). For weak acids it predicts that at acidic pH values ($pH < pK_a$) the predominant drop in both the neutral acid and the acid anion concentration should be located in the USLs, whereas in the alkaline pH range ($pH \gg pK_a$) the main drop in their concentrations should be located on the membrane itself. This prediction is not yet checked directly, although the measurements of the weak acid fluxes gave strong evidence in favor of the model. In recent years the microelectrode technique has been developed, making it possible to measure the concentration distribution of different ions near the surface of cellular membranes (Ammann, 1986). In the case of bilayer lipid membranes, the pH profiles induced in the unstirred layers by the permeation of weak acids are measured (Antonenko and Bulychev, 1991; Antonenko et al., 1993).

Ammonia has unique features among the whole class of weak electrolytes. It is a minute molecule that even lacks a convenient radiotracer. This hindered considerably the determination of the membrane permeability for ammonia. On the other hand, ammonium ion selective microelectrodes are easy to prepare now, because their main component (the ammonium cocktail) is commercially available. The aim of the present study is to investigate concentration profiles of ammonium and hydrogen ions by means of ion-selective microelectrodes under the conditions of a transmembrane ammonium gradient. These measurements, carried out at different bulk pH values, enable us to directly determine the BLM permeability for ammonia.

THEORY

Fig. 1 shows an example of calculated concentrations profiles of ammonia and ammonium ions for an intermediate case when both the membrane and the unstirred layers take part in the limitation of the transport process. Let us first consider a case in which the permeation of ammonia across

Received for publication 15 March 1996 and in final form 31 December 1996.

Address reprint requests to Dr. Y. N. Antonenko, Belozersky Institute of Physico-Chemical Biology, Moscow State University, Moscow 119899, Russia. Tel.: 70-95-939-53-60; Fax: +70-95-939-3181; E-mail: anton@mem.genebee.msu.su.

Dr. Denisov's present address is Department of Physiology and Biophysics, Cornell University Medical College, NY, NY 10021.

0006-3495/97/05/2187/09 $2.00

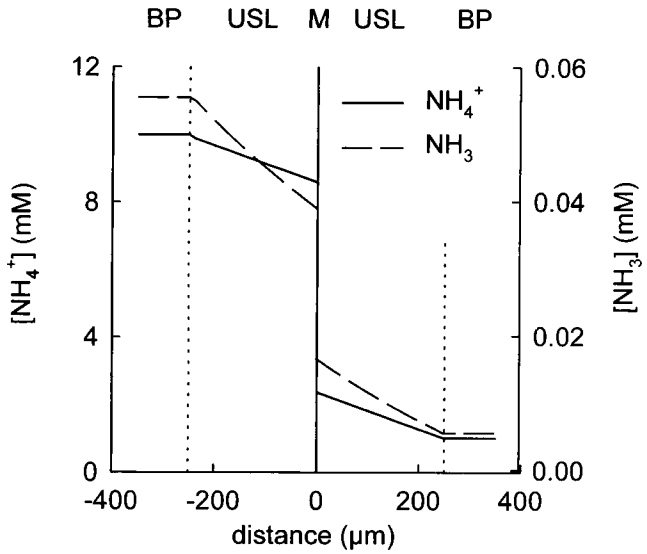

FIGURE 1 Local concentration shifts of ammonia (*dashed curves*) and ammonium ions (*solid curves*) within the unstirred layers (USLs) near a planar bilayer lipid membrane (M) and within the bulk phase (BP). The data were generated by the model described in the Theory section for the conditions 100 mM buffers with pK_a 6.2 and 8.2, pH 7.0, 10 mM ammonium ions in the left solution and 1 mM in the right, membrane permeability for ammonia 48×10^{-3} cm/s. pH shifts within the USLs were less than 0.1.

the BLM is assumed to proceed under the conditions of high buffer capacity of the medium, i.e., without pH changes in the unstirred layers. The concentration of ammonia under these conditions is proportional to the concentration of the ammonium ions in both unstirred layers and is determined by the pK_a value.

It is known that in the case of artificial planar bilayer lipid membranes, the membrane permeability for ammonium ions is lower by several orders of magnitude than for ammonia, and the process of its permeation is accompanied by proton binding (Walter and Gutknecht, 1986). The ammonium concentration profiles in the unstirred layers near the BLM can be used for the determination of the membrane permeability for ammonia. In fact, the membrane permeability for ammonia P^M is equal to the ratio of the transmembrane flux of ammonia and its concentration difference across the membrane.

$$P^M = J^M/\Delta C^M. \tag{1}$$

It is possible to calculate ΔC^M from the transmembrane difference of the ammonium ion concentrations determined by microelectrodes. The NH_3 flux across the membrane is equal to the sum of the NH_3 and NH_4^+ fluxes near the membrane, which can be computed from the NH_4^+ concentration profile according to

$$J^M_{NH_3} = -D_{NH_3}\frac{d[NH_3]}{dx} - D_{NH_4^+}\frac{d[NH_4^+]}{dx} = -D_{NH_4^+}\frac{d[NH_4^+]}{dx}(1+\alpha), \tag{2}$$

where D_{NH_3} and D_{NH_4} are the diffusion coefficients of NH_3 and NH_4^+, respectively, and $\alpha = 10^{(pH-pKa)}$. Simple considerations show that the permeability measurements should be carried out at acidic pH values to guarantee the accuracy required. Under these conditions, the NH_4^+ concentration near the BLM differs insignificantly from its bulk value. If the dissociation of ammonia proceeds much faster than its transport, equilibrium should be reached. Therefore, $\Delta C^M_{NH_3} = \Delta C^M_{NH_4}\,\alpha$ is true. The measured values of NH_4^+ concentrations at the *cis* and the *trans* sides in the immediate membrane vicinity can be expressed as

$$[NH_4^+]^{measured} = [NH_4^+]^{true} \pm E.$$

The absolute error E originates from the noise of the microelectrode (see Materials and Methods). The transmembrane difference $\Delta C^M_{NH_4^+}$ of the experimentally measured NH_4^+ concentrations must be expressed as

$$\Delta C^M_{NH_4^+} = [NH_4^+]^{meas}_{cis} - [NH_4^+]^{meas}_{trans} + E_{cis} + E_{trans}. \tag{3}$$

Because ΔC^M gets smaller at alkaline pH, the absolute error of the measurement can be even greater than the parameter itself (Eq. 3).

Instead of addressing the flux, a parameter not directly measured in the present work, the slope of the NH_4^+ profile is discussed in the following, because it is proportional to the flux and is easy accessible from the experimental data. At acidic pH values the NH_3 flux is determined by the membrane permeability according to Eq. 2. Therefore the slope of the NH_4^+ concentration profile $d[NH_4^+]/dx$ should not depend on the stirring conditions and should only be determined by P^M. On the contrary, in the alkaline pH range the slope should decrease with an increase in the width of the USLs, because the transport is limited by the diffusion through the unstirred layers. In the extreme case the membrane does not act as a barrier for the permeation, and the concentration drop is located in the unstirred layers exclusively.

In the present work, a previously published theoretical model of the permeation of a weak electrolyte across the USLs and the BLM is used (Antonenko et al., 1993). The model initially made for CH_3COOH takes into account both the reactivity of the weak base and its ability to diffuse. The following set of differential equations is used to numerically calculate the concentration profiles of the protonated and deprotonated forms of the weak electrolyte as well as the pH profile in the unstirred layers:

$$J_i = -D_i dc_i/dx, \quad i = 1, \ldots, 8. \tag{4}$$

This equation assumes that the electric field arising from ion diffusion through either USL is negligibly small:

$$dJ_i/dx = R_i(c); \qquad i = 1, \ldots, 8; \qquad c = (c_1, \ldots, c_8). \tag{5}$$

Here, J_i, D_i, $c_i(x)$ are, respectively, the flux, the diffusion coefficient, and the concentration of the ith species, where $1 = H^+$, $2 = NH_3$, $3 = NH_4^+$, $4 = OH^-$, $5 = A^{2-}$, $6 =$

AH^-, 7 = B, 8 = BH^+ (A and B are buffer molecules). $R_i(c)$ is the specific local rate of expenditure of the ith species in the chemical reactions

$$H^+ + NH_3 = NH_4^+; \quad H^+ + OH^- = H_2O; \tag{6}$$

$$H^+ + MES^{2-} = MES^-; \quad H^+ + Tris = TrisH^+. \tag{7}$$

At the membrane-water interface, the fluxes of all species are required to be equal to zero, except for J_2, so that

$$J_1 = J_3 = J_4 \ldots = J_8 = 0; \qquad J_2 = J. \tag{8}$$

Other boundary conditions are formulated by Antonenko et al. (1993). The numerical solutions are derived, assuming that the rates of chemical reactions (like dissociation/recombination of water, buffers, and ammonia) are very high compared to the rate of diffusion through the USL, so that the local chemical equilibrium is maintained. The program can be given upon request (a diskette should be included).

It should be noted that the model uses the conventional approximation of the unstirred layer as a layer of a solution lacking convection, where mass-transfer processes proceed due to diffusion only (Pedley, 1983; Barry and Diamond, 1984). In this model the width of the USLs cannot be calculated. It should be treated as an external parameter to achieve the best fit of the experimental profiles (see Figs. 5 and 6).

MATERIALS AND METHODS

The BLMs were formed by a conventional method (Mueller et al., 1963) in a hole, 1.5 mm in diameter, of a diaphragm dividing a PTFE chamber. The membrane-forming solutions contained 20 mg diphytanoyl phosphatidylcholine (Avanti Polar Lipids) in 1 ml of *n*-decane (Merck), unless otherwise stated. The solution was agitated by magnetic bars (2 mm diameter, 3 mm length) or magnetic balls (3 mm in diameter).

Ammonium chloride was added to the buffer solutions surrounding the bilayer. Its concentration at the *cis* side of the membrane was higher than at the *trans* side. Ammonia flux accompanied by chemical reactions led to a pH gradient in the USLs. The latter was measured in terms of a potential difference between a pH microelectrode and a reference electrode, both placed in the buffer solution at the same side of the membrane, as described previously (Antonenko and Bulychev, 1991; Pohl et al., 1993). The voltages were recorded by a Keithley 617 electrometer and transferred to a personal computer via an IEEE interface. The sensitivity of the microelectrode measurements, which was limited by the noise from the electrode, was about 0.1 mV.

The pH sensors were made of glass capillaries containing antimony. After pulling, their tips had a diameter of about 5–10 μm. Ammonium ion selective microelectrodes were prepared with the help of an ammonium cocktail obtained from Fluka. The microelectrodes were moved perpendicular to the surface of the BLM by a hydraulic microdrive manipulator (Narishige). The touching of the membrane was detected with the help of a microscope. Because the velocity of the electrode motion was known (usually 2 μm/s), the position of the sensor relative to the membrane could be determined at any time.

Experimental NH_4^+ and pH profiles were reproducible. The most variable parameter was the width of the profiles; however, the variation did not exceed 8% under the particular stirring conditions. Each experiment was performed at least three times and typical examples were reported. For the quantitative measurements of the membrane permeability for ammonia (P^M), the statistical deviations are presented.

RESULTS

Fig. 2, *A* and *B*, shows the ammonium concentration profiles in the *trans* unstirred layers. An increase in the NH_4^+ concentration at the *cis* side (from 10 mM to 60 mM) induces an increasing shift of the NH_4^+ concentration near the surface of the *trans* side of the BLM. The growing difference between the bulk concentrations at both sides of the membrane is shown to be proportional to the slope of the concentration profile (Fig. 2 *A*, *inset*). The values of the slopes are calculated by a linear regression of the data presented in Fig. 2 *A* at a distance of 0–100 μm from the BLM (straight lines on Fig. 2 *A*).

The addition of cholesterol to the membrane-forming solution reduces the slope of the NH_4^+ concentration profile at pH 6.0 (Fig. 2 *B*). These experiments were done at high buffer capacity of the medium (30 mM) to diminish the influence of the pH shifts in the USLs. For example, the magnitude of the pH shift in Fig. 2 *B*, *curve 2*, was 0.04. Because cholesterol is known to reduce membrane permeability for nonelectrolytes (Orbach and Finkelstein, 1980), the reduction of the slope agrees well with the statement

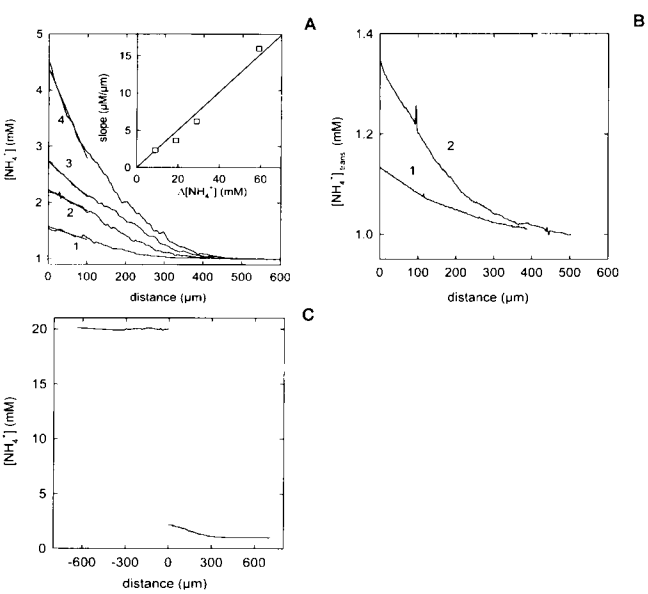

FIGURE 2 (*A*) NH_4^+ concentration profiles at the *trans* side of the BLM (ammonium bulk concentration at the *cis* side 10 mM, 20 mM, 30 mM, 60 mM, *curves 1, 2, 3, 4*, respectively). The solution was 20 mM Tris, 100 mM choline chloride, pH 7.5. The bulk concentration of NH_4Cl was 1 mM at the *trans* side. The rotation rate of the magnetic balls was 1.5 rotations/s. *Inset*: The dependence of the slope of the NH_4^+ concentration profiles on the difference of the NH_4^+ bulk concentrations at the opposite sides of the BLM. The slopes were obtained by a linear fit of the profiles within a distance of 100 μm from the membrane surface (*straight lines*). (*B*) NH_4^+ concentration profiles obtained within the unstirred layers for membranes made from diphytanoyl phosphatidylcholine (*curve 2*) and a 2:1 mixture of the lipid and cholesterol (*curve 1*). The solution was 30 mM MES, 100 mM choline chloride, pH 6.0. The NH_4Cl concentrations were 1 mM and 10 mM at the *trans* and *cis* sides, respectively. The rotation rate of the magnetic balls was 1.5 rotations/s. (*C*) NH_4^+ concentration profiles at both sides of the membrane at pH 7.5. The conditions were the same as in *A*. The NH_4^+ concentration was 20 mM at the *cis* side and 1 mM at the *trans* side.

made in the Theory section that in the acidic pH range the slope of the profile is determined by the membrane permeability for ammonia.

Fig. 2 *C* shows the NH_4^+ concentration profiles at both sides of the BLM at pH 7.5. If pH $\ll$ pK_a, it is hard to record changes of the NH_4^+ concentration within the *cis* unstirred layer, because the membrane itself acts as the predominant diffusion barrier. Voltage changes of the NH_4^+-selective electrode are in the range of the detection threshold under these conditions. At more alkaline pH values these changes are well pronounced (Figs. 5 and 6).

The permeation of NH_4^+ through the BLM is accompanied by proton transfer reactions in the unstirred layers, inducing pH shifts near the BLM. In a poorly buffered medium, the near-membrane pH changes are maximum (Antonenko et al., 1993). Fig. 3 shows pH profiles at the *trans* USL. In agreement with results reported previously (Antonenko and Bulychev, 1991), the increase in the transmembrane ammonium ion concentration gradient enhances the pH shifts near the BLM (Fig. 3).

Fig. 4 shows the effect of the buffer capacity of the medium on the pH shifts (*A*) and on the ammonium ion concentration profiles (*B*). The increase in the Tris concentration decreases the pH shift near the BLM considerably and increases the difference between the ammonium ion concentration in the immediate membrane vicinity and in the bulk. As was pointed out by Antonenko et al. (1993), the increase in the concentration of the buffer decreases the experimentally measured width of the pH profile. This effect is also observed with the NH_4^+ concentration profiles.

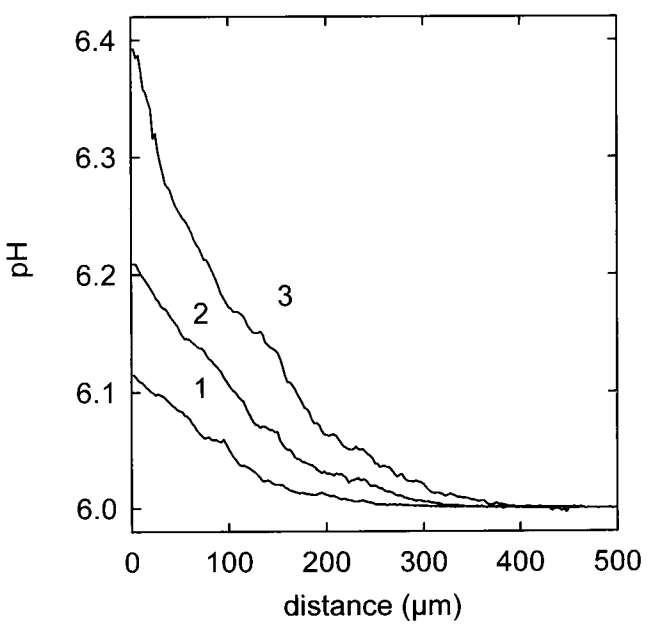

FIGURE 3 pH profiles at the *trans* side of the BLM at different NH_4Cl gradients across the BLM (5 mM *cis* and 0.5 mM *trans*, *curve 1*; 10 mM *cis* and 1 mM *trans*, *curve 2*; 20 mM *cis* and 2 mM *trans*, *curve 3*). The buffer solution was 1 mM MES, 100 mM choline chloride, pH 6.0. The rotation rate of the magnetic bars was 3 rotations/s.

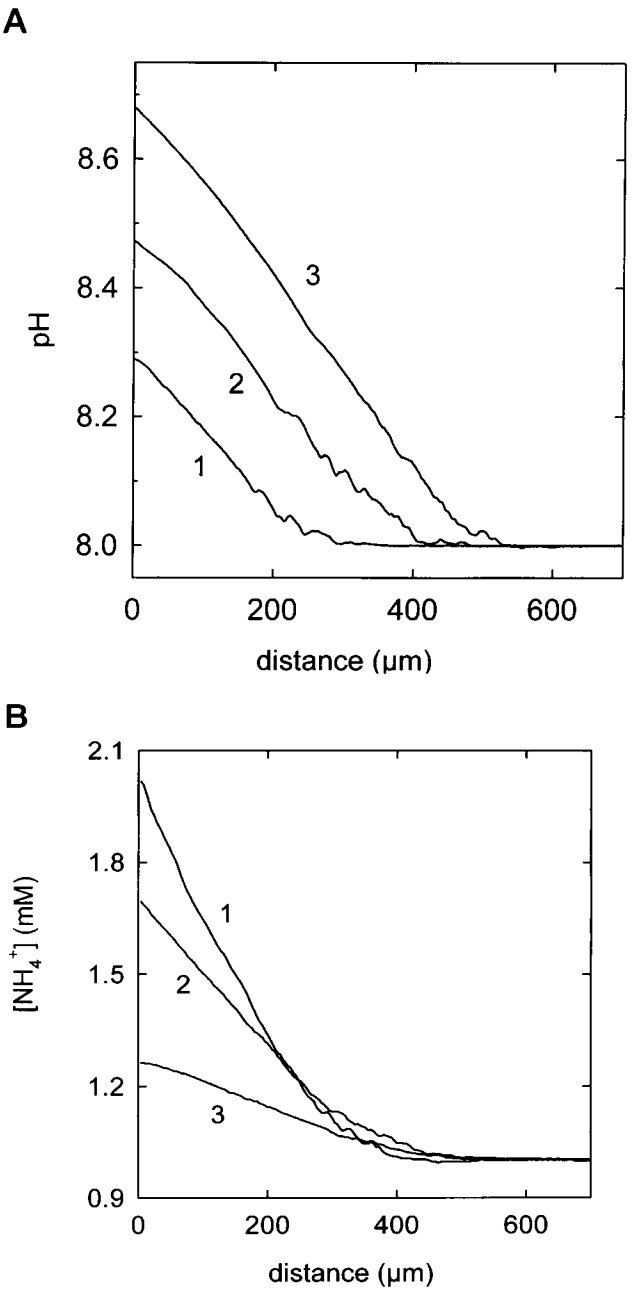

FIGURE 4 (*A*) pH profiles at the *trans* side of the BLM at different concentrations of Tris in the solution (10 mM, 5 mM, and 1 mM for *curves 1, 2, 3*, respectively). The solution also contained 100 mM choline chloride, pH 8.0. Other conditions were similar to Fig. 3, *curve 2*. (*B*) NH_4^+ ammonium concentration profiles were measured under the same conditions.

A series of pH and NH_4^+ concentration profiles recorded at different stirring rates is presented in Fig. 5. It is seen that both the pH and NH_4^+ concentration shifts are diminished because of an improvement of convection. The near-membrane slopes of the profiles depend poorly on the stirring conditions, in agreement with the statement that at acidic pH values the slope of the profiles is determined by the permeability of the membrane only. It is worth noting that the

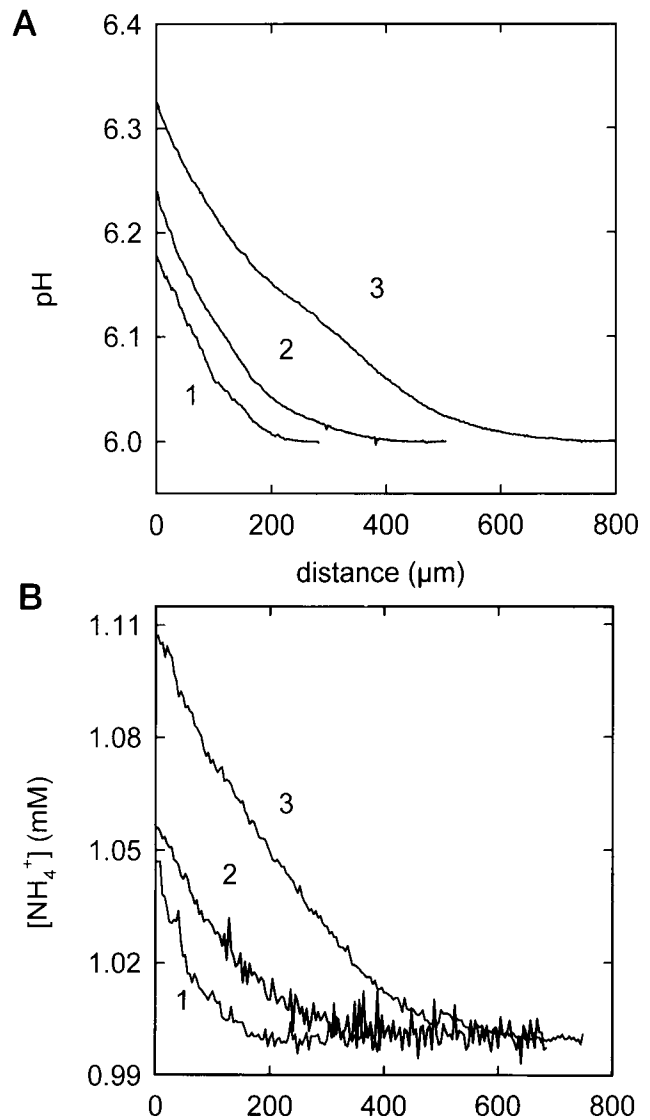

FIGURE 5 (*A*) pH profiles at the *trans* side of the BLM at different rotation rates of the magnetic bars (3 rotations/s, 1 rotation/s, 0.5 rotations/s, *curves 1, 2, 3*, respectively). The conditions were similar to Fig. 3, *curve 2*. (*B*) NH_4^+ ammonium concentration profiles measured under the same conditions.

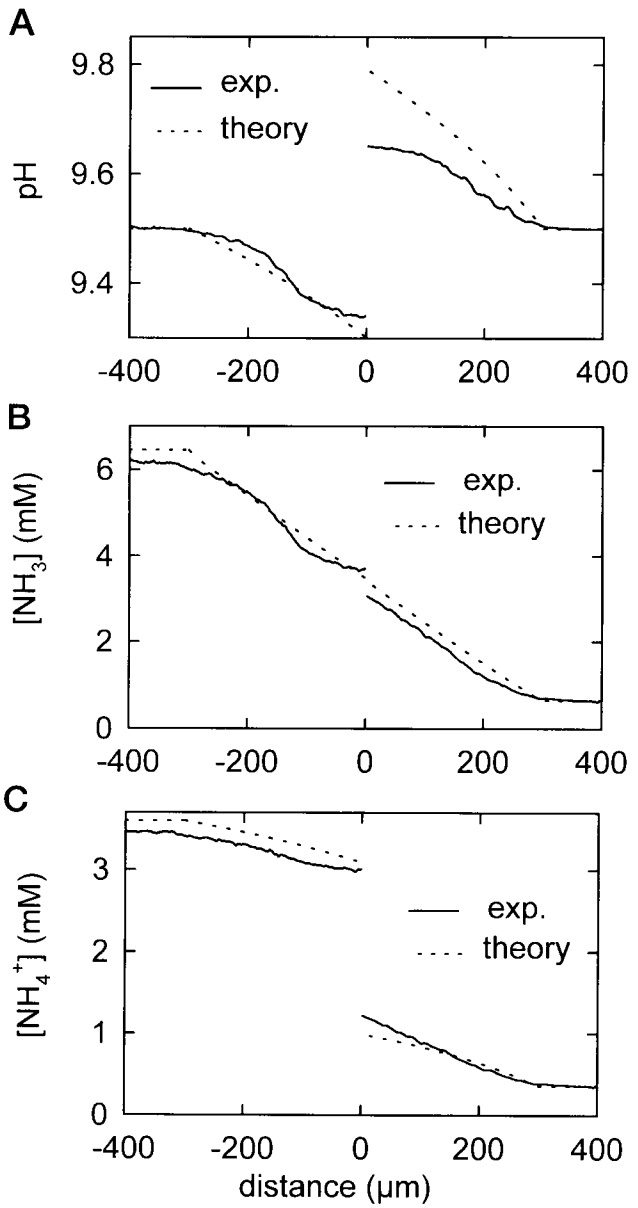

FIGURE 6 Experimental (*solid curves*) and theoretical (*dashed curves*) concentration profiles of hydrogen ions (*A*), ammonia (*B*), and ammonium ions (*C*) at both sides of the BLM at pH 9.5. The ammonia concentration was calculated from the ammonium and hydrogen ion concentrations, assuming a pK_a value of 9.25. The gradient of NH_4Cl was 10 mM at the *cis* side and 1 mM at the *trans* side. The solution contained 10 mM Tris, 10 mM β-alanine, and 100 mM choline chloride. The rotation rate of the magnetic balls was 1.5 rotations/s.

concentration shift near the membrane in Fig. 2 *B* is higher than in Fig. 4 because of the higher buffer capacity in the former case.

On the other hand, at alkaline pH values the permeation of ammonia should be determined by diffusion across the USLs and there should not be a transmembrane ammonia concentration drop. The ammonia concentration can be calculated easily if the ammonium and hydrogen ion concentrations are known (the pK_a of NH_3 is assumed to be 9.25). Figs. 6 and 7 show concentration profiles of ammonium (Figs. 6 *C* and 7 *C*) and hydrogen (Figs. 6 *A* and 7 *A*) ions and the calculated concentration profiles of ammonia (Figs. 6 *B* and 7 *B*) measured at pH 9.5 (Fig. 6) and 10.5 (Fig. 7). It is seen from Figs. 6 and 7 that under these conditions the NH_3 concentrations at opposite sides of the BLM surface are similar. Theoretical concentration profiles calculated according to Eqs. 4–8 are represented by dashed lines (Figs. 6 and 7).

It is worth noting that the rate of the motor rotation that drives the magnetic bars should be varied cautiously. At high rotation rates (more than 4 rotations/s) the NH_4^+ concentration profiles observed (Fig. 8) differ greatly from the ones shown in Fig. 5. The slope of the concentration profile

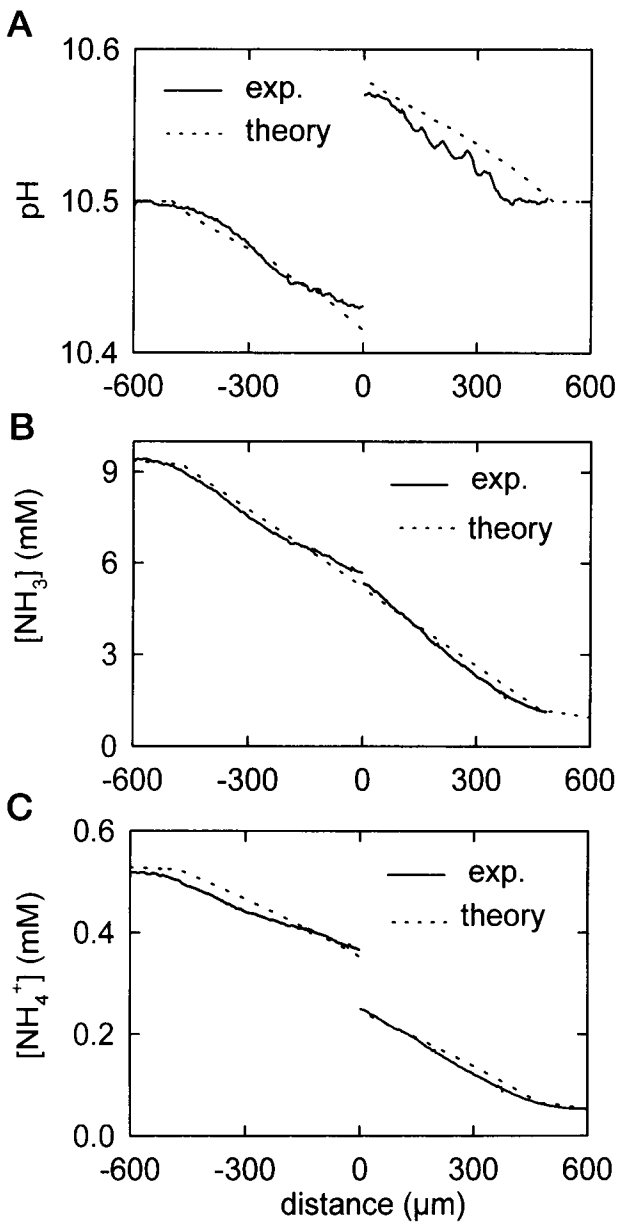

FIGURE 7 Experimental (*solid curves*) and theoretical (*dashed curves*) concentration profiles of hydrogen ions (*A*), ammonia (*B*), and ammonium ions (*C*) at both sides of the BLM at pH 10.5. For all other conditions, see Fig. 6.

near the BLM decreases considerably. The same phenomenon is observed if the magnetic bars are taken out of the cell. Obviously it is not possible to attribute the effect to fluid flows induced by the rotation of magnetic bars. Moreover, when the experiment is repeated under the conditions of incomplete spreading of the BLM, a strong shaking of the membrane is observed by a light microscope. Thus the phenomenon of slope reduction is attributed to the BLM shaking accompanied by fluid flow in the immediate membrane vicinity. Because this observation has a certain experimental and theoretical significance, we report it here, although we do not control the membrane shaking.

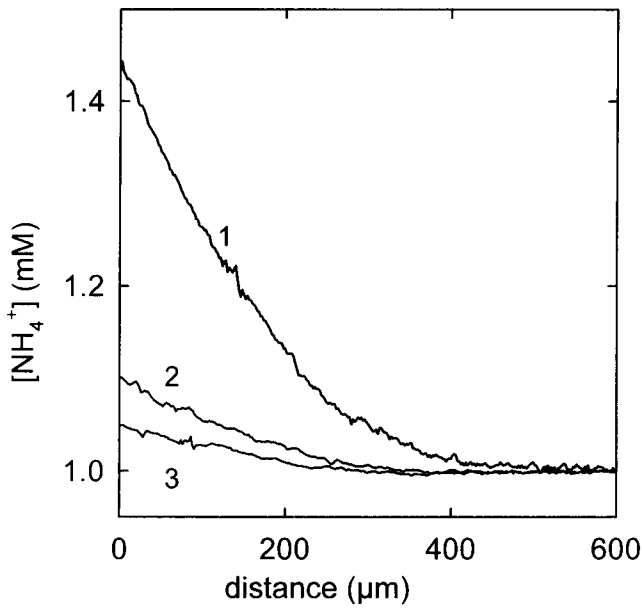

FIGURE 8 The effect of a high rotation rate of the motor driving the magnetic balls (1.5 rotations/s, 4 rotations/s, and 5 rotations/s, *curves 1, 2, 3*, respectively) on the NH_4^+ concentration profile at the *trans* side of the BLM. The solution consisted of 10 mM MES, 100 mM choline chloride, pH 6.5. The concentration of NH_4Cl was 10 mM at the *cis* side and 1 mM at the *trans* side.

DISCUSSION

Experimentally measured NH_4^+ concentration profiles can be used for the calculation of the membrane permeability for ammonia; the highest precision is attained at acidic pH values. These conditions are realized, for example, in Fig. 2 *B*. Calculating the slopes of the profiles as described for the inset of Fig. 2 *A*, and assuming an ammonia diffusion coefficient of 1.957×10^{-5} cm^2/s (Lide, 1993), the membrane permeability for NH_3 is determined. In the case of diphytanoyl phosphatidylcholine (PC), a value of $(48 \pm 5) \times 10^{-3}$ cm/s (M $\pm$ SD, $N = 8$) is obtained. A 2:1 mixture of diphytanoyl PC and cholesterol, PC from soybeans, and a 2:1 mixture of PC from soybeans and cholesterol give $(21 \pm 10) \times 10^{-3}$ ($N = 9$) cm/s, $(52 \pm 4) \times 10^{-3}$ ($N = 5$) cm/s, and $(16 \pm 5) \times 10^{-3}$ ($N = 6$) cm/s, respectively. These results are in reasonable agreement with earlier estimated values (Antonenko and Yaguzhinsky, 1982; Walter and Gutknecht, 1986). For PC 130×10^{-3} cm/s (Walter and Gutknecht, 1986) and for a 2:1 mixture of PC and cholesterol, 20×10^{-3} cm/s (Antonenko and Yaguzhinsky, 1982) were reported. It should be noted that for unexplained reasons the value of P^M undergoes a great deviation in the presence of cholesterol. In contrast, the P^M values in the absence of cholesterol vary comparatively little.

Qualitatively, the measured concentration profiles of ammonium ions are well described by the standard model of weak electrolyte permeation across membranes (Jackson, 1987; Gutknecht and Tosteson, 1973), if the buffer capacity exceeds the concentration of the weak base by at least one order of magnitude. In fact, the model predicts that within

the acidic pH interval the NH_3 diffusion through the membrane must be the limiting transport step, and the main decrease in the NH_3 concentration should occur within the membrane. The experiments confirm this prediction, as seen from the comparison of Fig. 2 *C* and Fig. 7. For example, in the experiments of Fig. 5, the alteration of the NH_4^+ concentration is about 0.1 mM within the *trans* USL, whereas it is nearly 9 mM across the membrane. At alkaline pH values the transport through the unstirred layer should be the limiting step of the total permeation process. Indeed, at pH 10.5 the main drop in the NH_4^+ concentration profile is situated in the USLs and only a minor part in the membrane (Fig. 7). As far as we know, this is the first time that concentration profiles have been directly measured and compared with the predictions of the model. It has been checked so far by indirect measurements of the total weak electrolyte fluxes across the membrane only.

As it can be seen from a comparison of Figs. 5 *B* and 2 *B*, a decrease in the buffer capacity of the medium from 30 mM to 1 mM leads to a decrease in the amplitude of the NH_4^+ concentration shift near the surface of the BLM from 1.34 mM to 1.06 mM under similar stirring conditions. This corresponds to the decrease in the ammonia flux across the membrane by 4.1 times, as calculated from the profile slopes. The pH near the surface of the membrane under similar stirring conditions was reduced from 6.23 to 6.04 as the buffer concentration increased. Fig. 4 shows directly the effect of pH shifts near the membrane on the permeation of weak bases across the BLM. As expected, under the condition of a low buffer capacity, the experimental model used previously is not valid. Instead, the more sophisticated model described in the second part of the Theory section should be used; it takes into account the local pH changes in the unstirred layers. This model gives 1.27 mM and 1.077 mM for the amplitudes of the NH_4^+ concentration shifts and 4.51 for the flux ratio under these conditions (Figs. 5 *B* and 2 *B*). The calculations were carried out with the same set of parameters as used previously (Antonenko et al., 1993). A value of 48×10^{-3} cm/s is assumed for P^M. The solution contained two buffers with a pK_a value of 8.2 (Tris) and 6.2 (2-(*N*-morpholino)ethanesulfonic acid, MES). At the alkaline pH range β-alanine is substituted for MES (pK_a 10.2).

The impact of pH shifts within the unstirred layers on transport kinetics can be estimated from the ratio of the ammonia/ammonium concentration and the buffer capacity. Theoretical calculations (compare Eqs. 4–8) confirmed by experiments (Figs. 2–4) show that an x-fold increase in the ammonium ion concentration increases the value of pH changes approximately x times. The pH shift returns to its initial value if the concentration of the buffer is also increased x times.

The membrane permeability for ammonia can also be estimated from the data of pH shifts of Fig. 3 using the theoretical model. The following values for P^M fit well the pH shifts 20, 26, and 55×10^{-3} cm/s for curves 1, 2, and 3, respectively. These values are close to that obtained from ammonium ion concentration profiles. However, they vary considerably. Although the experimental error can be decreased significantly by multiple repetitions of the measurements, a large systematic error remains. The computations are based on a set of pK_a and D values that may be shifted with salt concentration or temperature. Small variations in the buffer concentrations create an additional error. The model-independent calculation of P^M from NH_4^+ profiles recorded at a high buffer capacity lacks this disadvantage.

Even if the transmembrane transport is exclusively determined by permeation across the USL, the pH profiles calculated from the model are close to experimental ones. For example, experimentally measured (theoretically calculated) values of pHs at the surface of the BLM for curves 1, 2, and 3 (Fig. 4 *A*) are 8.29 (8.36), 8.47 (8.45), and 8.68 (8.63), respectively.

The dependency of the concentration/pH shifts near the membrane on the width of the unstirred layers is predicted well by the model. Experimentally measured (theoretically calculated) values of concentration shifts at the surface of the BLM for curves 1, 2, and 3 (Fig. 4) are 1.044 (1.060) mM, 1.055 (1.068) mM, and 1.10 (1.077) mM, respectively, for ammonium ions and 6.18 (6.27), 6.24 (6.31), and 6.32 (6.35), respectively, for pH. The width of the unstirred layers is estimated with 144 μm, 218 μm, and 346 μm from the slopes of the NH_4^+ concentration profiles within a distance of 100 μm near the surface of the BLM for curves 1, 2, and 3, respectively.

The model works well also if the transmembrane gradient and/or the pH of the medium is varied (Figs. 2 *A*, 5, and 6). In fact, for the conditions of Fig. 2 *A* the theoretical (experimentally measured) shifts are 1.80 (1.65) mM, 2.16 (2.18) mM, 2.41 (2.72) mM, and 2.94 (4.48) mM, respectively. A good agreement between theoretical and experimental curves is to be seen from Figs. 6 and 7, where both experimental and theoretical concentration profiles (*dashed curves*) are plotted.

The maximum deviation between measured and calculated profiles is observed for the *trans* pH profile at pH 9.5 (Fig. 6 *A*). Because of the proton-transfer reactions in the USLs, the calculated concentration profiles diverge from linearity, as expected from the standard model, in which the concentration distribution within the USL is governed solely by diffusion.

The quantitative divergence between the model and the experiment may be attributed to the approximation of the USL as a solution layer where convective flows are absent and mass transfer is carried out by diffusion only. This limitation manifests itself in a sharp edge of the theoretical profile at the boundary of the USL/bulk phase that is absent in the experimental profiles.

In the absence of convective flows and under the conditions of high buffer capacity of the medium, the NH_4^+ concentration profiles should be linear (Fig. 1). On the other hand, it is shown that in the case of H^+ concentration profiles they may be well approximated by an empirical

function (Pohl et al., 1993):

$$[NH_4^+] = ([NH_4^+]_{membrane} - [NH_4^+]_{bulk})e^{-x/\delta} + [NH_4^+]_{bulk}. \quad (9)$$

We compare the linear and uniexponential regression of the experimental NH_4^+ profiles, using the data of Fig. 2 *A*. Calculations show that even in the case of small distances from the BLM (<100 μm), the exponential function gives a fit that is similar to or better than the linear function. δ remains nearly constant and equal to 145 μm. Thus it can be concluded that for the case of NH_4^+ concentration profiles the uniexponential function is a good approximation of the experimentally measured concentration profiles, as it is in the case of proton concentration profiles (Pohl et al., 1993).

Fig. 8 presents the effect of BLM shaking on the NH_4^+ concentration profiles in the USL. The shaking leads to an unexpected result, namely to a sharp decrease in the profile slope. These measurements are carried out in an acidic environment (pH 6.0), in which the slope of the profile should be determined by the membrane permeability for ammonia (see Theory section) and should therefore be independent of the stirring conditions (Fig. 5). From the comparison of the profiles in Figs. 5 and 8, the conclusion can be drawn that under the conditions of membrane shaking the convective fluid flow cannot be neglected, even in the immediate membrane vicinity, i.e., that the conventional model of the unstirred layer is not valid under these conditions. Recently it was shown that shaking stimulates solute fluxes into the intestine epithelium (Levitt et al., 1992). The concentration profiles observed in our study underline the observation that the movement of the membrane itself is the most effective way to distort the unstirred layer.

The membrane permeability for ammonia depended significantly on the kind of cell membrane (Kikeri et al., 1989; Ritchie and Gilson, 1987; Hamm et al., 1985; Tsuruoka et al., 1993; Singh et al., 1995). Along with very permeable membranes, there are other examples, such as apical membranes from renal tubule cells, that have an ammonia permeability that is even lower than the permeability for ammonium ions (Kikeri et al., 1989). The increase in the membrane permeability for ammonium ions can easily be accomplished by the formation of NH_4^+ ion channels, whereas a way to make at least the phospholipid part of the membrane impermeable to NH_3 is hard to imagine. For example, as is shown in the present paper, the presence of cholesterol in the membrane reduces its permeability only 2.5 times. It should be mentioned in this respect that the values of the BLM permeabilities for nonelectrolytes measured on decane-containing membranes and solvent-free membranes differ insignificantly (Walter and Gutknecht, 1984), and therefore the values of P^M reported in the present work should not be influenced by the presence of decane in our BLMs. We suppose that the system described in the present work can be used not only for the particular study of ammonia permeability through the phospholipid part of biological membranes, but for the study of weak base or acid transport in general. Even if no microsensor for the substance of interest (acid or base) is available, the microelectrode technique is applicable, because with the help of the sophisticated theoretical model, the desired information can be calculated from pH profiles alone. However, the accuracy of this approach is limited because of the uncertainty of the equilibrium and diffusion constants and the buffer concentrations that may occur.

The authors are indebted to Dr. S. M. Saparov for technical assistance.

The work was partially supported by the Deutscher Akademischer Austauschdienst.

REFERENCES

Ammann, D. 1986. Ion-Selective Microelectrodes. Principles, Design and Application. Springer-Verlag, Berlin, Heidelberg, New York, Tokyo.

Antonenko, Y. N., and A. A. Bulychev. 1991. Measurements of local pH changes near bilayer lipid membrane by means of a pH microelectrode and a protonophore-dependent membrane potential. Comparison of methods. *Biochim. Biophys. Acta.* 1070:279–282.

Antonenko, Y. N., G. A. Denisov, and P. Pohl. 1993. Weak acid transport across bilayer lipid membrane in the presence of buffers—theoretical and experimental pH profiles in the unstirred layers. *Biophys. J.* 64: 1701–1710.

Antonenko, Y. N., and L. S. Yaguzhinsky. 1982. Generation of potential in lipid bilayer membranes as a result of proton-transfer reactions in the unstirred layers. *J. Bioenerg. Biomembr.* 14:457–465.

Barry, P. H., and J. M. Diamond. 1984. Effects of unstirred layers on membrane phenomena. *Physiol. Rev.* 64:763–972.

Gutknecht, J., and D. C. Tosteson. 1973. Diffusion of weak acids across lipid bilayer membranes: effects of chemical reactions in the unstirred layers. *Science.* 182:1258–1261.

Hamm, L. L., D. Trigg, D. Martin, C. Gillespie, and J. Buerkert. 1985. Transport of ammonia in the rabbit cortical collectory tubule. *J. Clin. Invest.* 75:478–485.

Jackson, M. J. 1987. Weak electrolyte transport across biological membrane. *In* Membrane Physiology. T. E. Andreoli and J. F. Hoffman, editors. Plenum Medical Books, New York.

Kikeri, D., A. Sun, M. L. Zeidel, and S. C. Hebert. 1989. Cell membranes impermeable to NH_3. *Nature.* 339:478–480.

Levitt, M. D., J. K. Furne, and D. G. Levitt. 1992. Shaking of the intact rat and intestinal angulation diminish the jejunal unstirred layer. *Gastroenterology.* 103:1460–1466.

Lide, D. R., editor. 1993. CRC Handbook of Chemistry and Physics, 74th Ed. CRC Press, Boca Raton. 5–90.

Mueller, P., D. O. Rudin, H. Ti Tien, and W. C. Wescott. 1963. Methods for the formation of single bimolecular lipid membranes in aqueous solution. *J. Phys. Chem.* 67:534–535.

Orbach, E., and A. Finkelstein. 1980. The nonelectrolyte permeability of planar lipid bilayer membranes. *J. Gen. Physiol.* 75:427–436.

Pedley, T. J. 1983. Calculation of unstirred layer thickness in membrane transport experiments. *Q. Rev. Biophys.* 16:115–150.

Pohl, P., Y. N. Antonenko, and E. Rosenfeld. 1993. Effect of ultrasound on the pH profiles in the unstirred layers near planar bilayer lipid membranes measured by microelectrodes. *Biochim. Biophys. Acta.* 1152: 155–160.

Ritchie, R. J., and J. Gilson. 1987. Permeability of ammonia and amines in *Rhodobacter sphaeroides* and *Bacillus firmus*. *Arch. Biochem. Biophys.* 258:332–341.

Singh, S. K., H. J. Binder, J. P. Geibel, and W. F. Boron. 1995. An apical permeability barrier to NH_3/NH_4^+ in isolated, perfused colonic crypts. *Proc. Natl. Acad. Sci. USA.* 92:11573–11577.

Tsuruoka, S., M. Takeda, K. Yoshitomi, and M. Imai. 1993. Cellular geterogeneity of ammonium ion transport across the basolateral membrane of the hamster medullary thick ascending limb of Henle's loop. *J. Clin. Invest.* 92:1881–1888.

Walter, A., and J. Gutknecht. 1984. Monocarboxylic acid permeability through lipid bilayer membranes. *J. Membr. Biol.* 77:255–264.

Walter, A., and J. Gutknecht. 1986. Permeabilities of small nonelectrolytes through lipid bilayer membranes. *J. Membr. Biol.* 90: 207–217.

Xiang, T. X., and B. D. Anderson. 1993. Diffusion of ionizable solutes across planar lipid bilayer membranes—boundary-layer pH gradients and the effect of buffers. *Pharm. Res.* 11:1654–1661.